Supplementary Information (SI) for Materials Horizons.
This journal is © The Royal Society of Chemistry 2026

Supplementary Information for

Piezoelectric [trimethylchloromethyl ammonium][$CdCl_3$] microrods/PVC composites for high-fidelity ultrasound detection in the mid-frequency range

Guan-Zhi Wang, Yong-Ji Gong, Chen Zhao, Rui Wang, Xu-Kai Niu, Xue-Qian Wei, Tian-Yi Yang, Hai-Run Yang, Zhi-Gang Li*, Wei Li, Xian-He Bu

School of Materials Science and Engineering & State Key Laboratory of Elemento-Organic Chemistry, Nankai University, Tianjin 300350, China

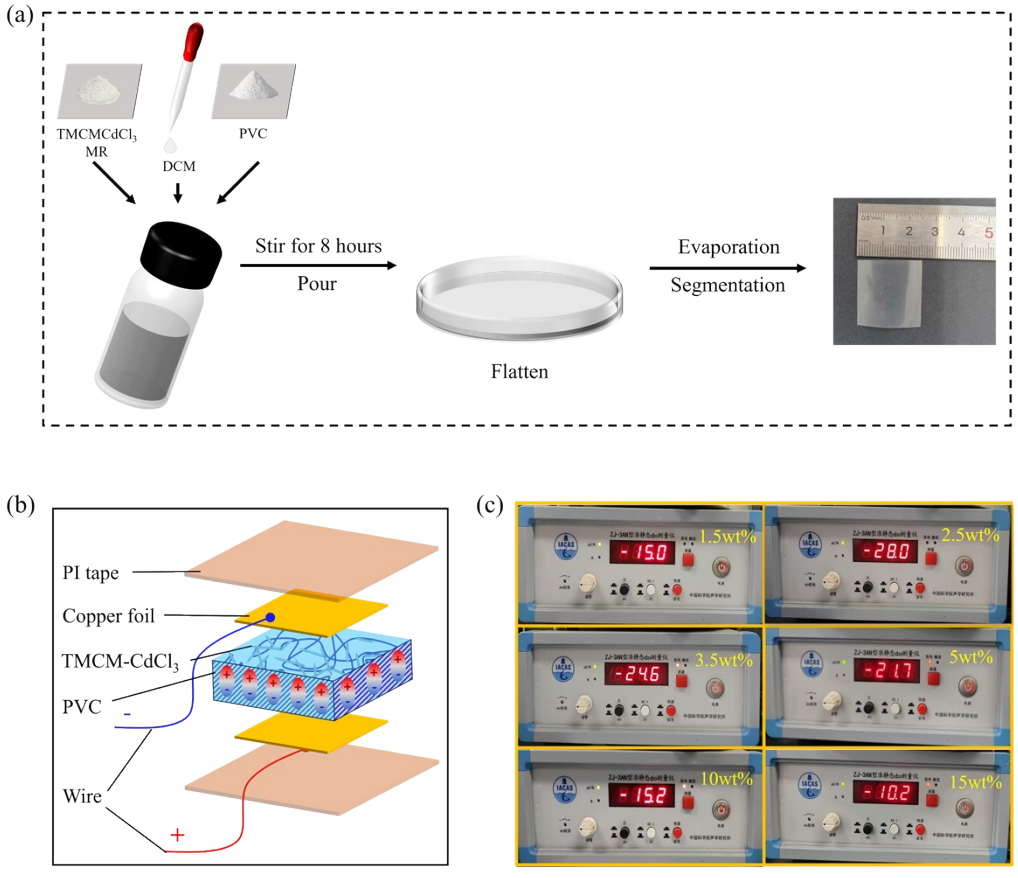

Fig. S1 (a) Schematic illustration of the preparation of $TMCMCdCl_3$ MRs/PVC composite film. (b) Schematic illustration of $TMCMCdCl_3$ MRs/PVC composite film device. (c) Original d_{33} figures of composite film devices with different $TMCMCdCl_3$ MRs concentration.

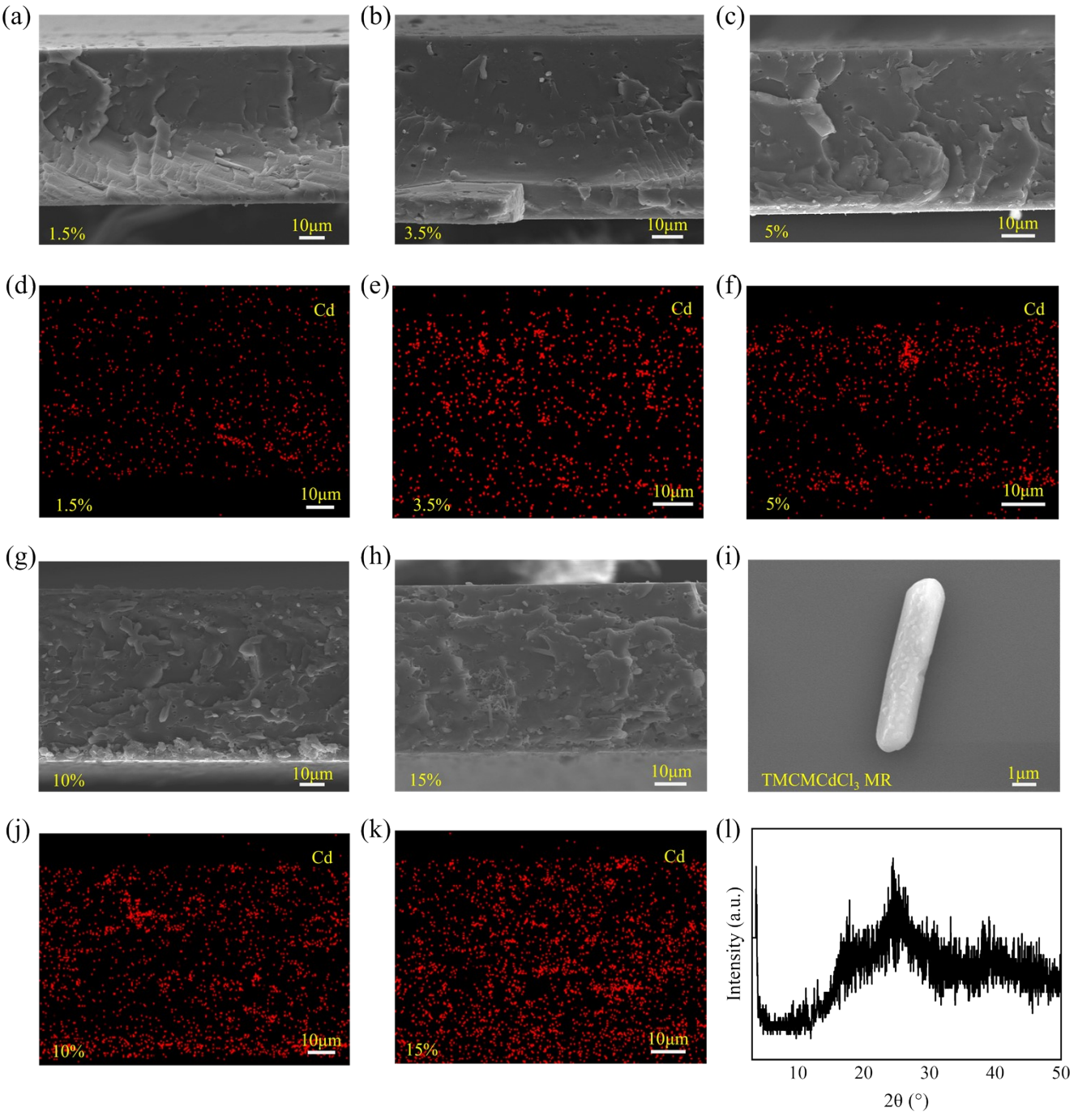

Fig. S2 SEM images of TMCM-$CdCl_3$ MRs/PVC composite films with different loadings: (a) 1.5 wt.%, (b) 3.5 wt.%, (c) 5 wt.%, (g) 10 wt.%, and (h) 15 wt.%. Corresponding elemental mapping images of (d) 1.5 wt.%, (e) 3.5 wt.%, (f) 5 wt.%, (j) 10 wt.%, and (k) 15 wt.% composite films. (i) SEM image of a single TMCM-$CdCl_3$ MR. (l) XRD pattern of a pure PVC film.

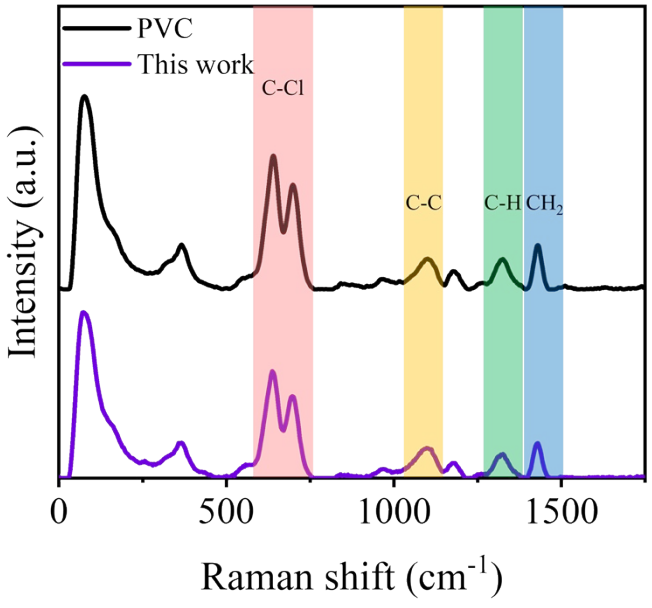

Fig. S3 Raman spectra of pure PVC film and α-film focusing in the range of 0-1750 cm^{-1}.

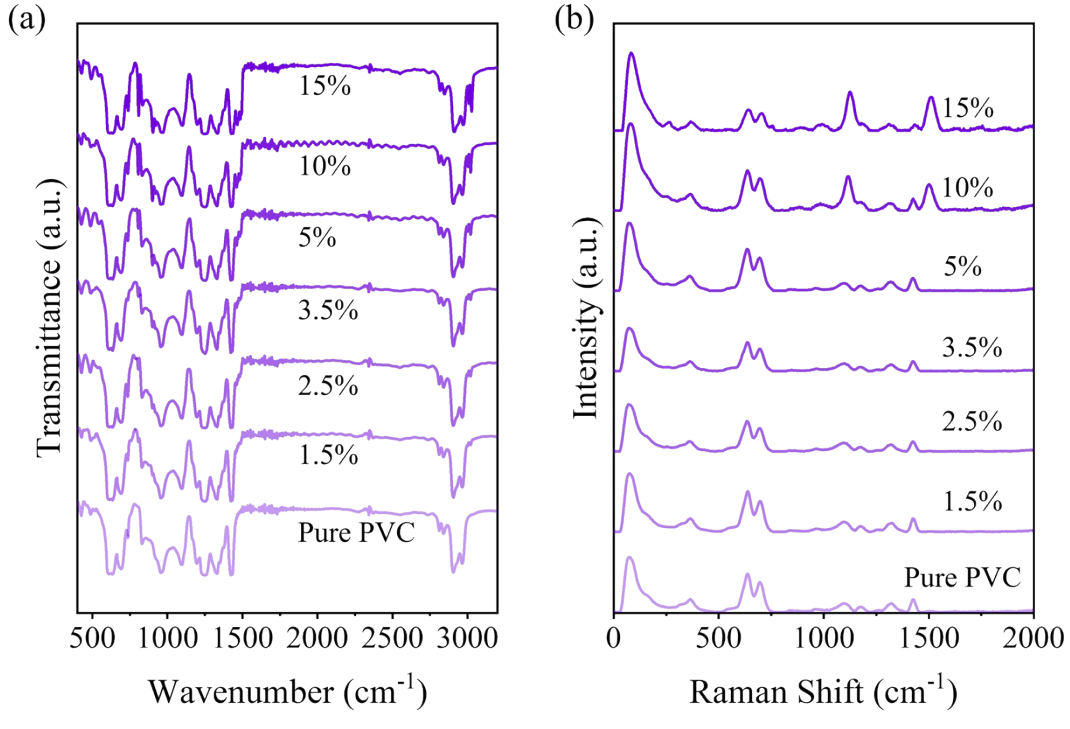

Fig. S4 Infrared (a) and Raman spectra (b) of pure PVC film and α-film in the range of 0-1750 cm^{-1}

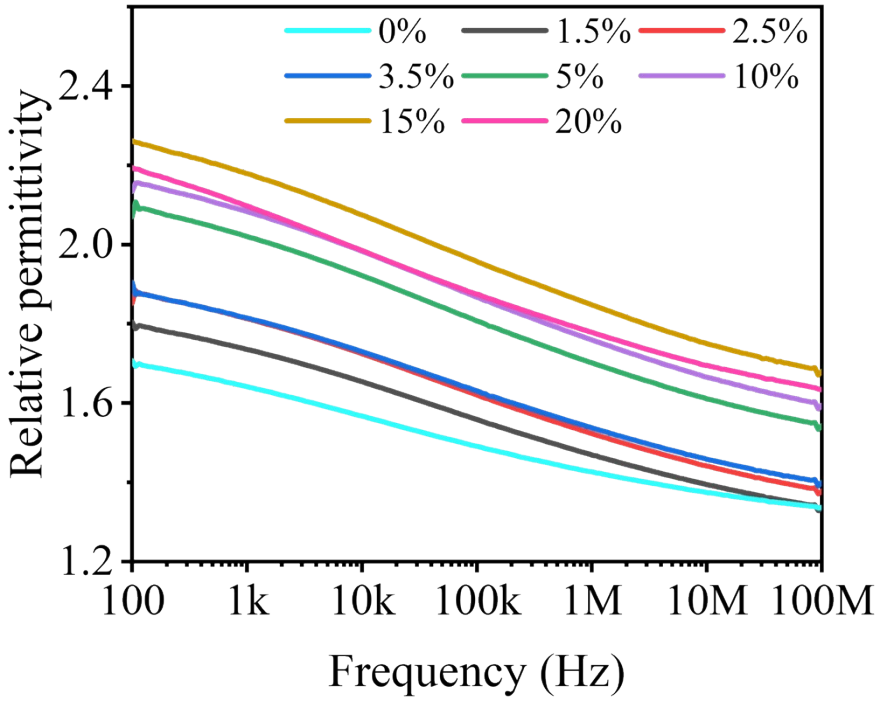

Fig. S5 The ε_r of composite films with different concentrations of TMCM-$CdCl_3$ MRs.

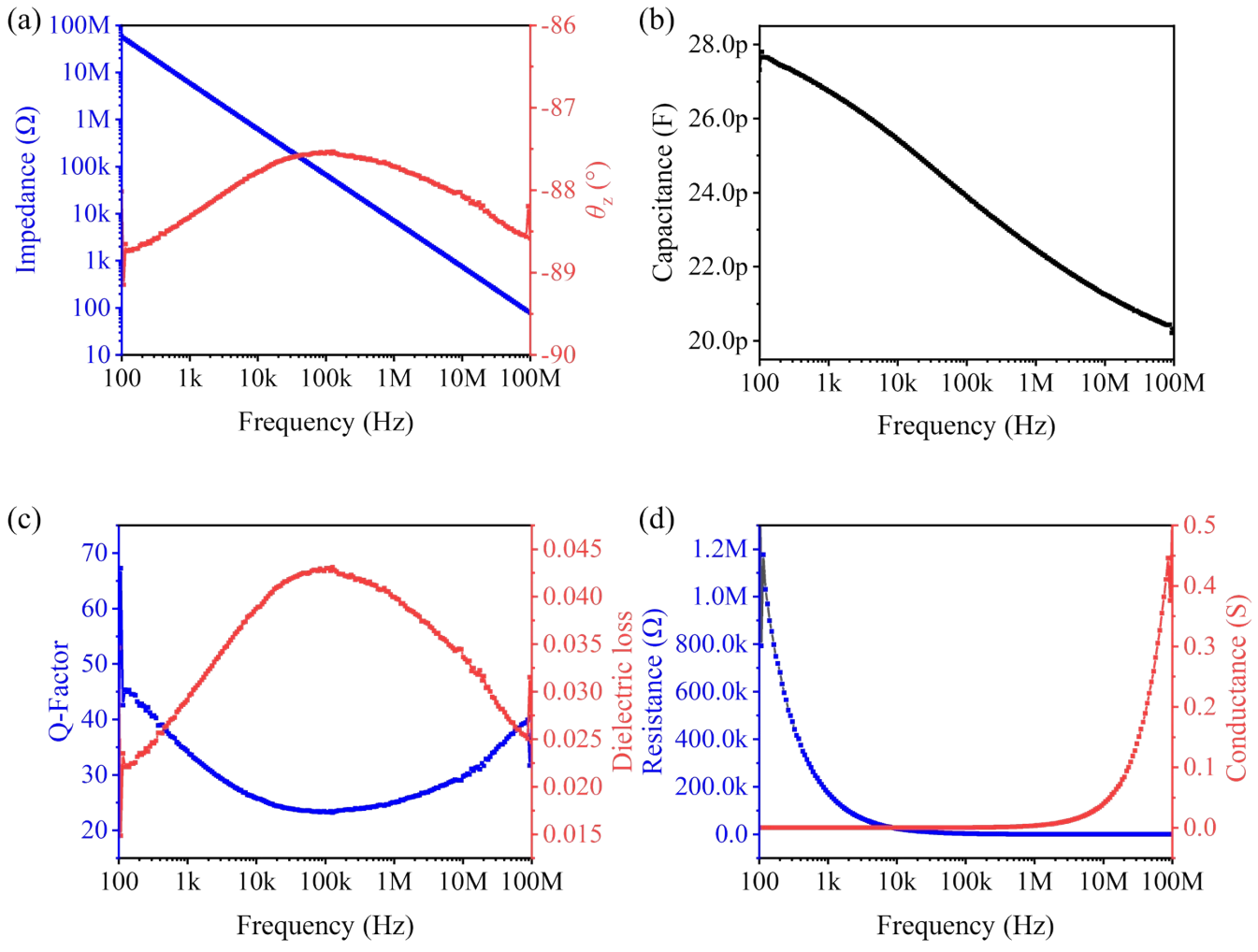

Fig. S6 Frequency-dependent electrical characteristics of the optimal 2.5 wt.% TMCM-$CdCl_3$ microrods/PVC composite film device, including (a) impedance magnitude and phase angle, (b) capacitance, (c) quality factor (Q) and dielectric loss (D, or tan δ), and (d) resistance and conductance.

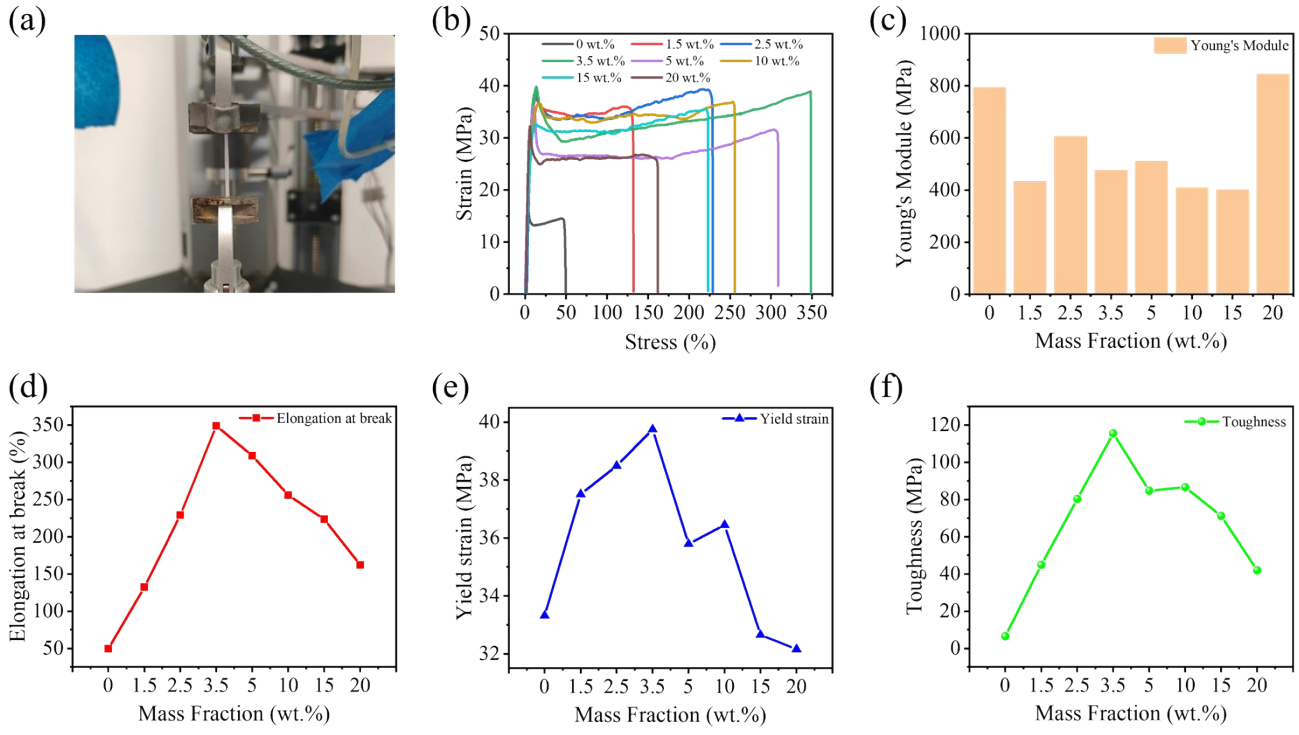

Fig. S7 Tensile properties of pure PVC and composite films with different mass fractions. (a) Optical photographs during tensile testing; (b) stress–strain curves; (c) Young's modulus; (d) elongation at break; (e) yield strain; (f) toughness of pure PVC and composite films with different mass fractions.

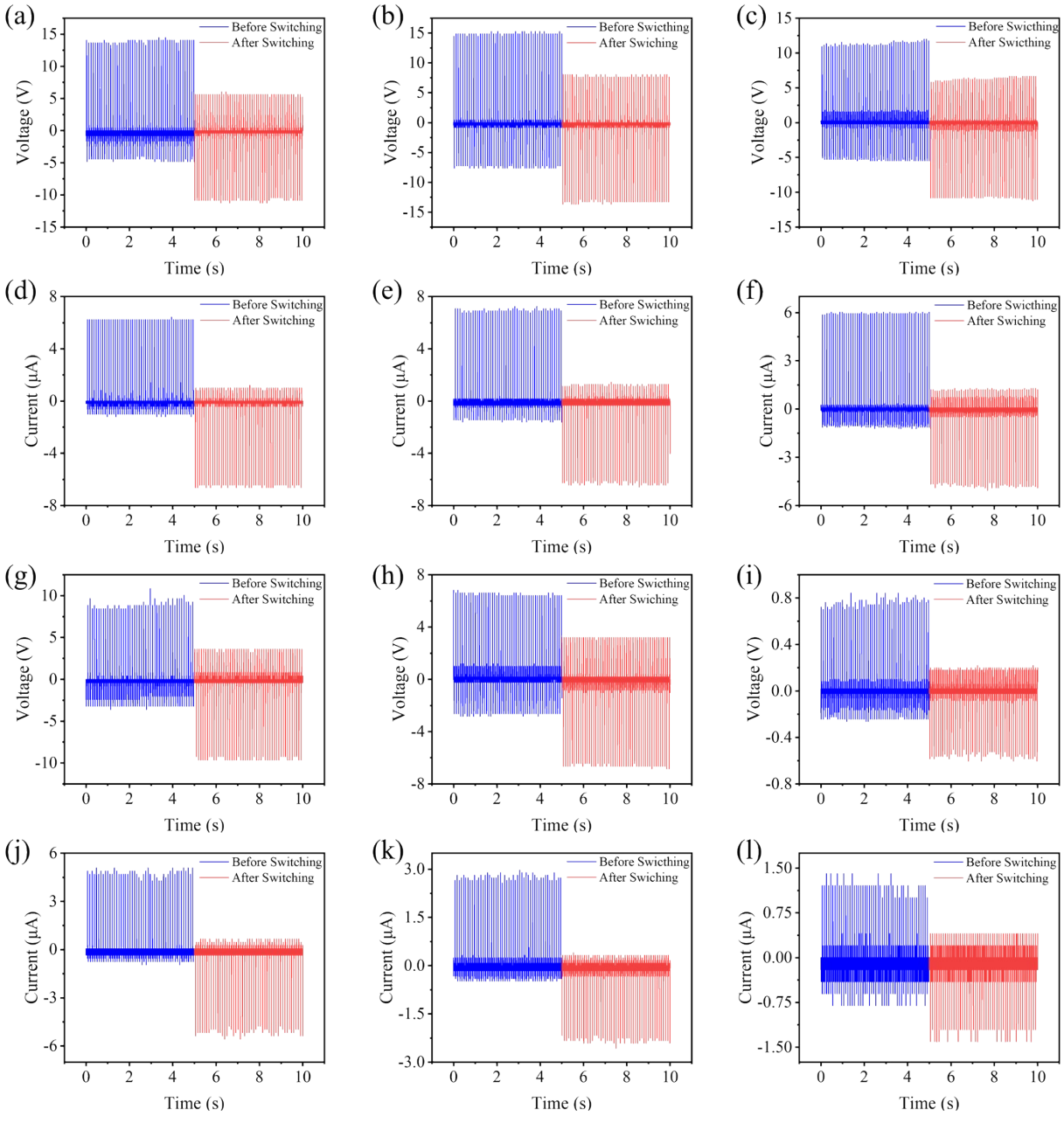

Fig. S8 The piezoelectric performances of TMCMCdCl$_3$ MRs/PVC composite film devices with different concentration under a constant force of 5 N and a frequency of 10 Hz. The V_{oc} performance before switching and after switching of PVC-based composite film devices with (a) 1.5wt. %, (b) 3.5wt. %, (c) 5wt.%, (g) 10wt.%, (h) 15wt.% TMCMCdCl$_3$ MRs. The I_{sc} performance before switching and after switching of PVC-based composite film devices with (d) 1.5wt. %, (e) 3.5wt. %, (f) 5wt.%, (j) 10wt.%, (k) 15wt.% TMCMCdCl$_3$ MRs. The (i) V_{oc} and (l) I_{sc} of pure PVC film device before and after switching.

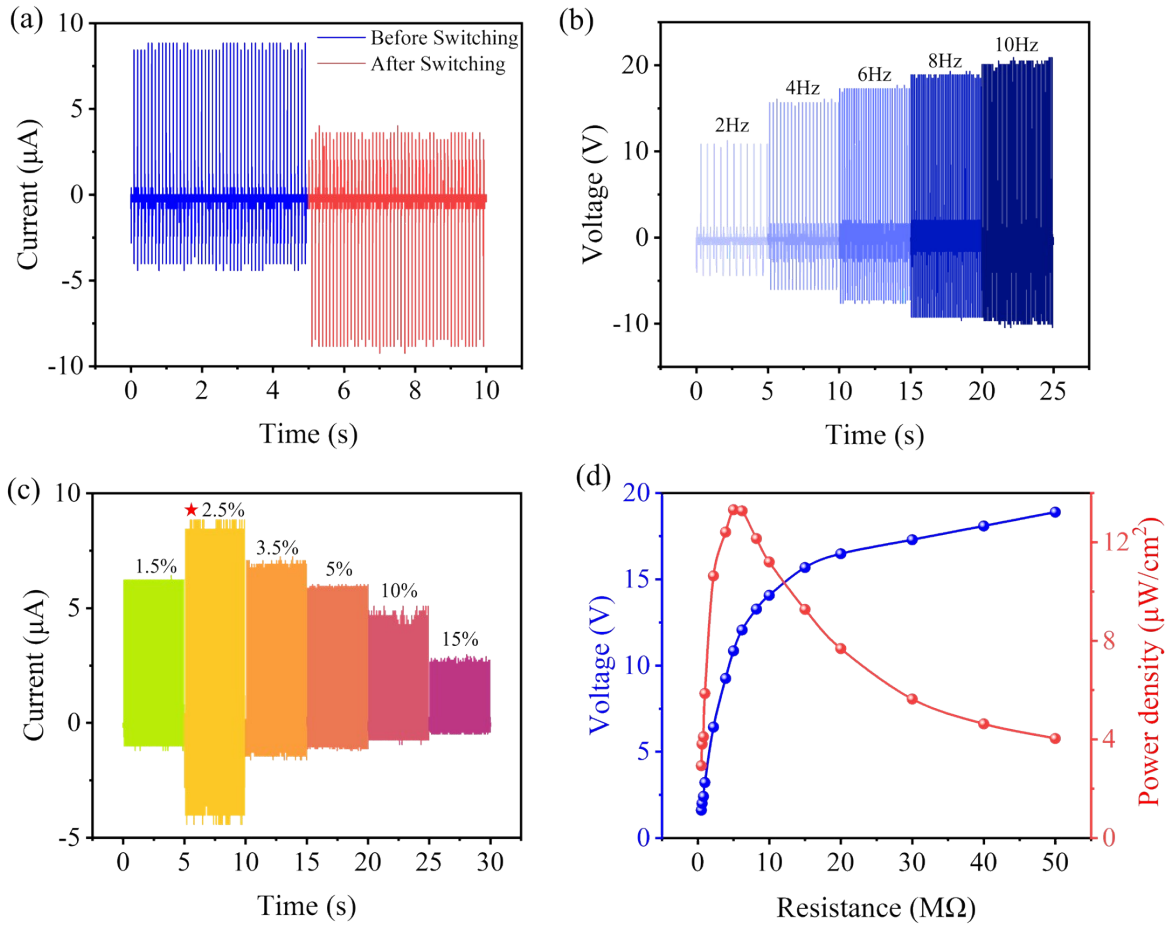

Fig. S9 The piezoelectric energy harvesting performance of TMCM-$CdCl_3$ MRs/PVC composite film devices. (a) I_{sc} performance of the α-film device. (b) V_{oc} of the α-film device at a stimulus force of 5 N and different frequencies. (c) I_{sc} of composite film devices with different TMCM-$CdCl_3$ MR concentration. (d) V_{oc} and power density of the α-film device under different load resistances.

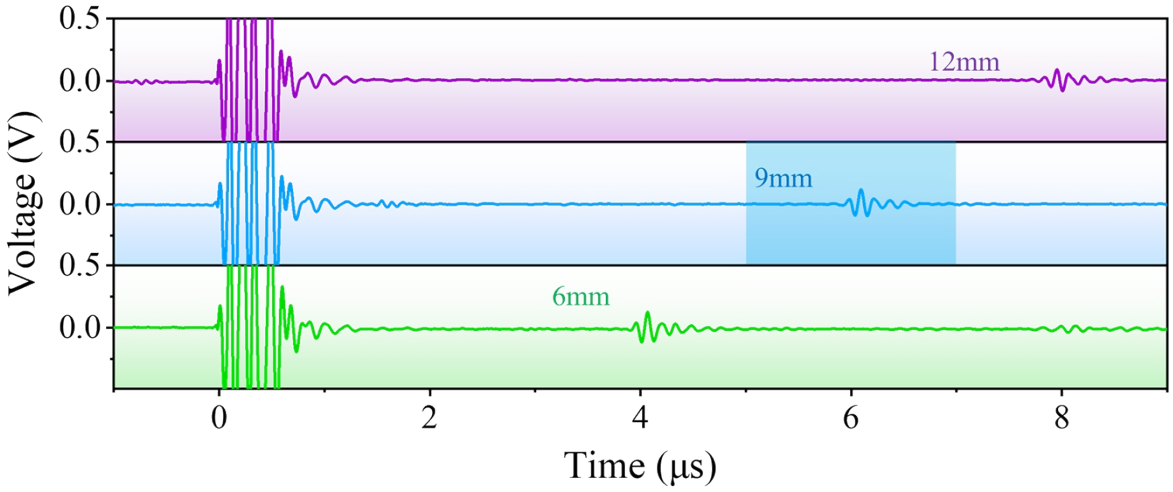

Fig. S10 Characteristic signals collected from *α*-film device under 10 MHz ultrasound excitation, with acoustic source distances of 12, 9, and 6 mm, respectively.

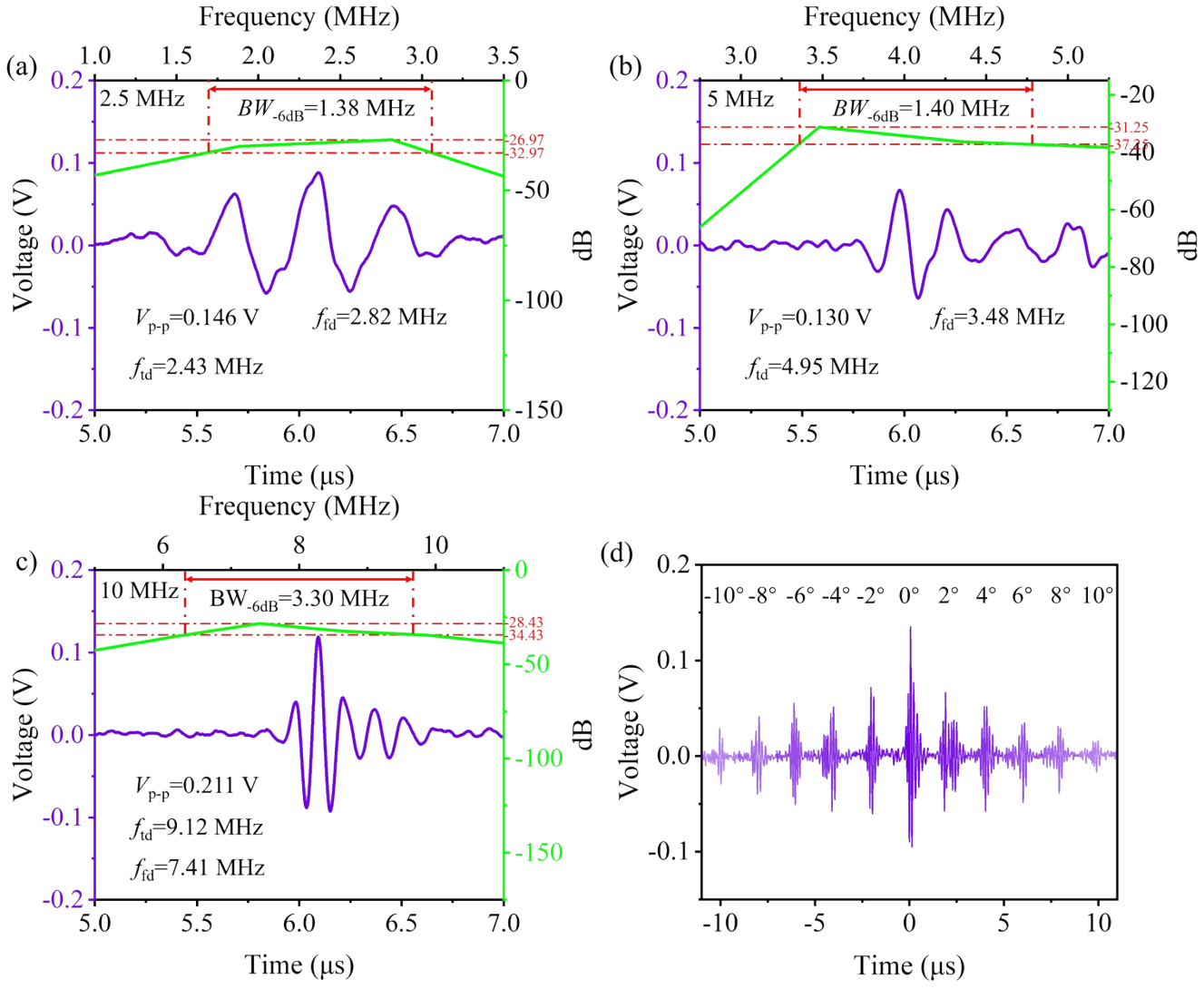

Fig. S11 Ultrasound detection signals and FFT-based spectral analysis of the *α*-film device. Excitation frequencies: (a) 2.5 MHz, (b) 5 MHz, and (c) 10 MHz (corresponding to the highlighted region in Fig. S13). (d) Ultrasound detection responses at different incident angles under 10 MHz excitation.

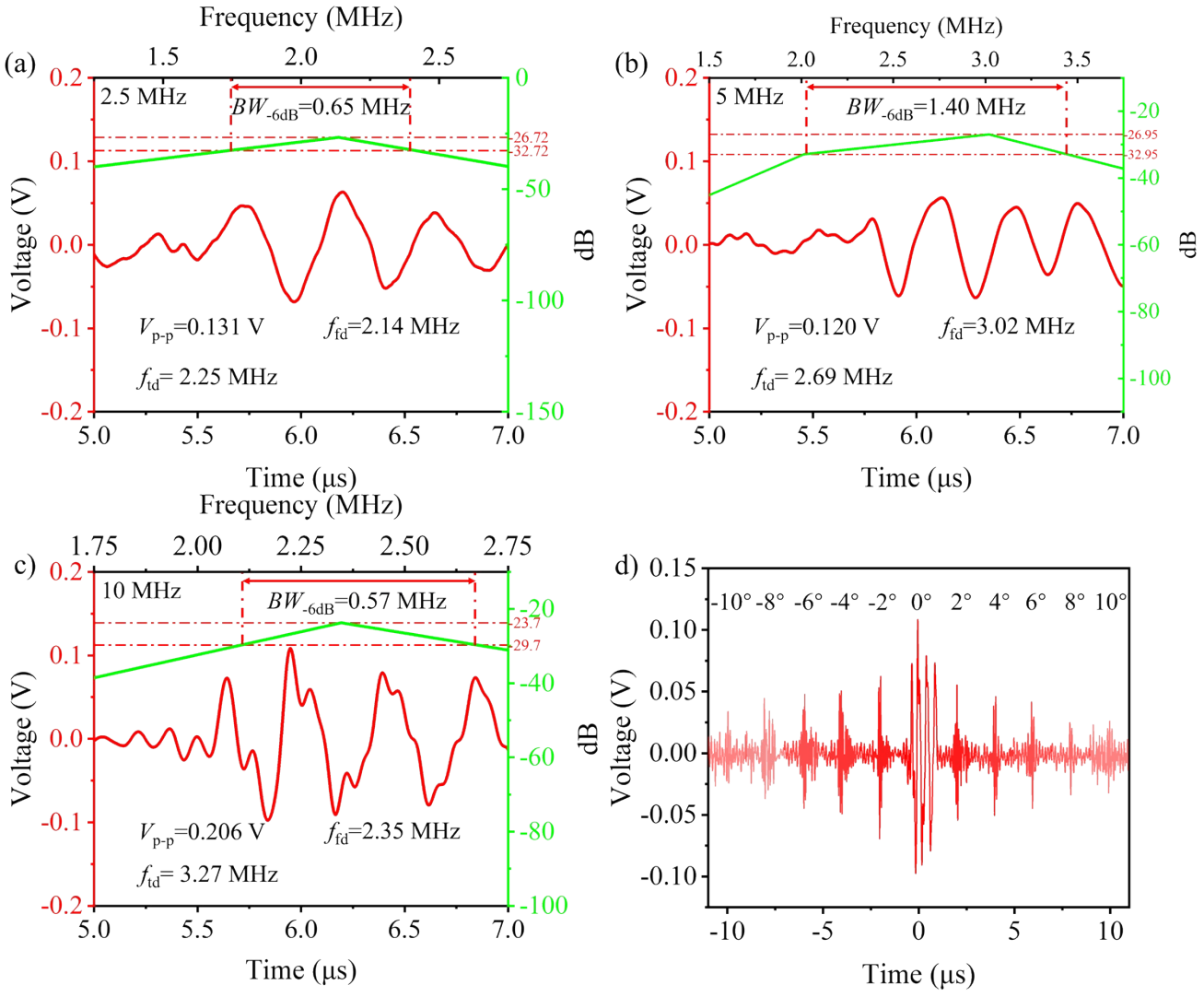

Fig. S12 Ultrasound detection signals and FFT-based spectral analysis of commercial PZT ceramics. Excitation frequencies: (a) 2.5 MHz, (b) 5 MHz, (c) 10 MHz, (d) Ultrasound detection responses at different incident angles under 10 MHz excitation.

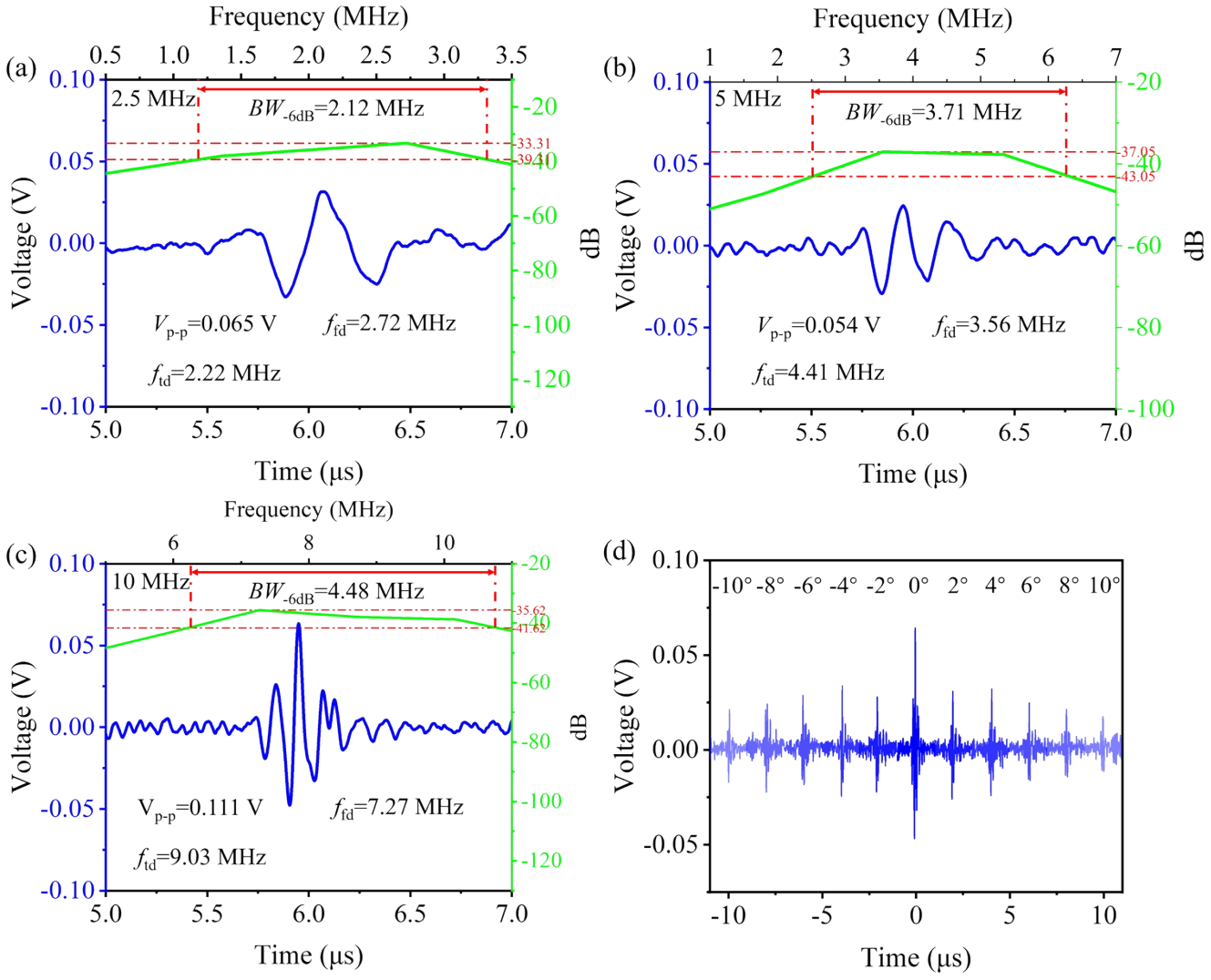

Fig. S13 Ultrasound detection signals and FFT-based spectral analysis of commercial PVDF. Excitation frequencies: (a) 2.5 MHz, (b) 5 MHz, and (c) 10 MHz. (d) Ultrasound detection responses at different incident angles under 10 MHz excitation.

.

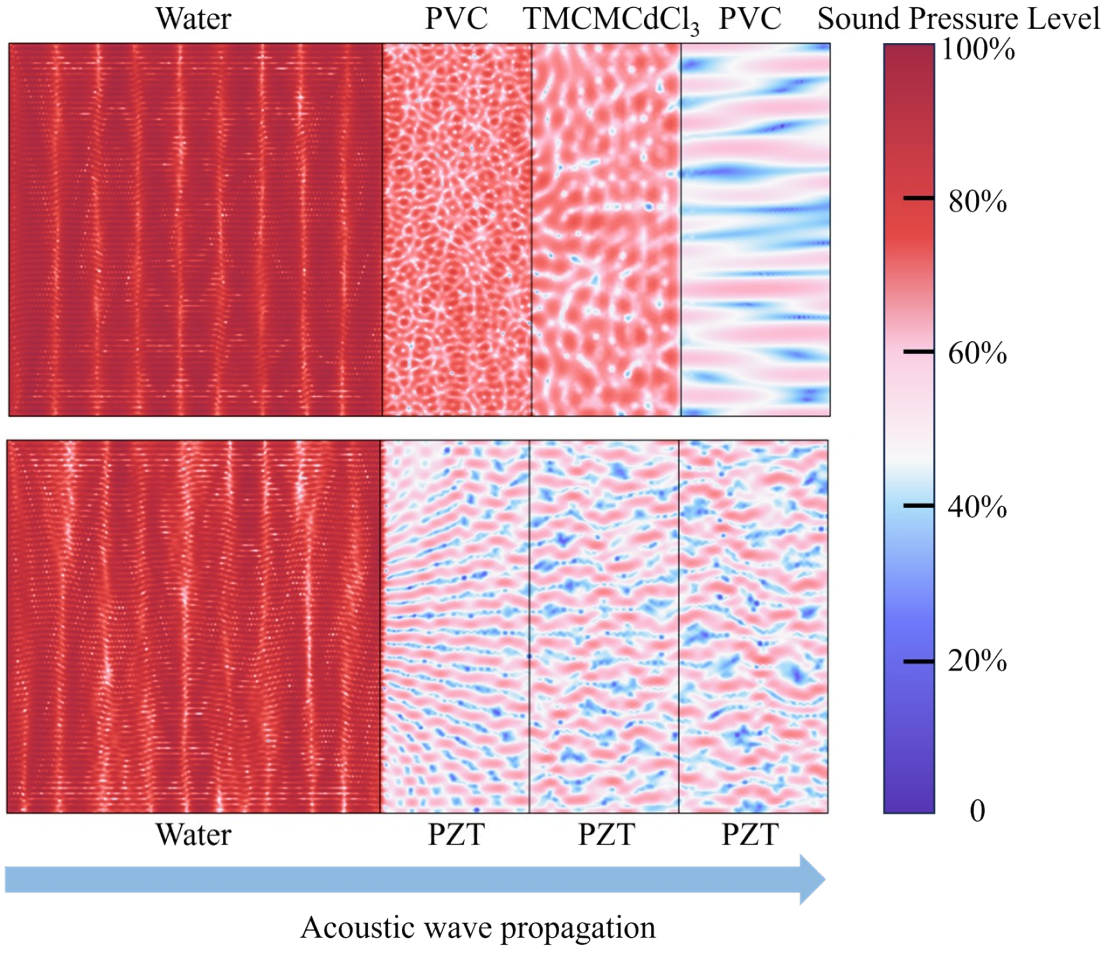

Fig. S14 Finite element method simulation of ultrasonic wave propagation in water–device systems, comparing the *α* composite film device and commercial PZT ceramic.

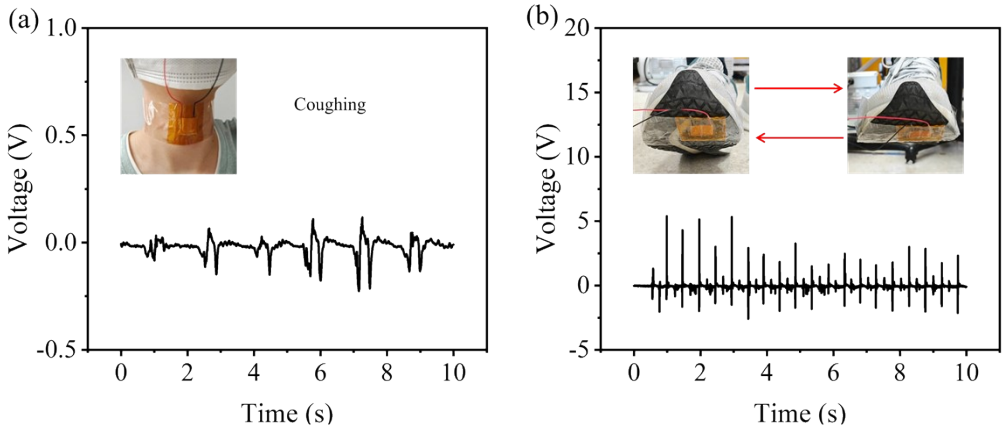

Fig. S15 Characterization of motion sensing performances. Schematic illustrations and corresponding voltage signals generated by (a) coughing, (b) tiptoe jumping.

Table S1: The -6 dB bandwidth of commercial PVDF, PZT and the composite film under 2.5, 5, and 10 MHz excitation frequencies.

	PVDF	PZT	This work
2.5 MHz	2.12 MHz	0.65 MHz	1.38 MHz
5 MHz	3.71 MHz	1.40 MHz	1.40 MHz
10 MHz	4.48 MHz	0.57 MHz	3.30 MHz